



# Water vapor absorption spectroscopy and validation tests of databases in the far-infrared (50–720 cm<sup>-1</sup>). Part 1: Natural water



M. Toureille<sup>a</sup>, A.O. Koroleva<sup>a,b</sup>, S.N. Mikhailenko<sup>c,d</sup>, O. Pirali<sup>e,f</sup>, A. Campargue<sup>a,\*</sup>

<sup>a</sup> Univ. Grenoble Alpes, CNRS, LIPhy, 38000 Grenoble, France

<sup>b</sup> Institute of Applied Physics, Russian Academy of Sciences, Nizhny Novgorod, Russia

<sup>c</sup> V.E. Zuev Institute of Atmospheric Optics, SB, Russian Academy of Science, 1, Academician Zuev square, 634055 Tomsk, Russia

<sup>d</sup> Climate and Environmental Physics Laboratory, Ural Federal University, 19, Mira av., 620002 Yekaterinburg, Russia

<sup>e</sup> SOLEIL Synchrotron, L'Orme des Merisiers, Saint-Aubin 91192, Gif-Sur-Yvette, France

<sup>f</sup> Université Paris-Saclay, CNRS, Institut des Sciences Moléculaires d'Orsay, 91405 Orsay, France

## ARTICLE INFO

### Article history:

Received 10 June 2022

Revised 11 July 2022

Accepted 18 July 2022

Available online 20 July 2022

### Keywords:

Water vapor

Far infrared

Rotational spectrum

Water isotope

## ABSTRACT

The rotational spectrum of water vapor in natural isotopic abundance has been recorded by high resolution ( $\approx 0.001 \text{ cm}^{-1}$ ) Fourier transform spectroscopy at the AILES beam line of the SOLEIL synchrotron. The room temperature absorption spectrum has been recorded between 50 and  $720 \text{ cm}^{-1}$  using five pressure values up to 7 mbar and an absorption pathlength of 151.75 m. Line parameters were retrieved for the five recorded spectra and then combined in a global list of 2867 water lines with line intensity ranging between a few  $10^{-26}$  and  $10^{-19} \text{ cm}^2/\text{molecule}$ . 454 of the measured lines are newly observed by absorption spectroscopy. The spectral calibration based on a statistical matching with about 700 accurate reference line positions allows for line center determinations with an accuracy of  $5 \times 10^{-5} \text{ cm}^{-1}$  for well isolated lines of intermediate intensity.

The large spectral coverage, the achieved position accuracy and sensitivity of the constructed line list make it valuable for validation tests of the current spectroscopic databases. Six water isotopologues ( $\text{H}_2^{18}\text{O}$ ,  $\text{H}_2^{16}\text{O}$ ,  $\text{H}_2^{17}\text{O}$ ,  $\text{HD}^{18}\text{O}$ ,  $\text{HD}^{16}\text{O}$ , and  $\text{HD}^{17}\text{O}$ ) were found to contribute to the spectrum. The line position comparison to the recent HITRAN2020 spectroscopic database and to the W2020 line lists of  $\text{H}_2^{16}\text{O}$ ,  $\text{H}_2^{17}\text{O}$  and  $\text{H}_2^{18}\text{O}$ , [Furtenbacher et al. J. Phys. Chem. Ref. Data 49 (2020) 043103; <https://doi.org/10.1063/5.0030680>] shows an overall very good agreement. Nevertheless, a number of significant deviations are observed. Part of them has an amplitude largely exceeding the W2020 claimed error bars. On the basis of the experimental data at disposal for the main isotopologue (1310 transitions), the best agreement is achieved with the positions calculated using the effective Bending–Rotation Hamiltonian [Coudert et al. J Mol Spectrosc 2014;303:36–41. <https://doi.org/10.1016/j.jms.2014.07.003>].

© 2022 Elsevier Ltd. All rights reserved.

## 1. Introduction

The present work is devoted to an experimental study of the high resolution absorption spectrum of natural water vapor in the far infrared region (FIR) between 50 and  $720 \text{ cm}^{-1}$ . It follows a recent study of the rotational spectrum of water vapor highly enriched in  $^{18}\text{O}$  in the same region [1]. In fact, the  $^{18}\text{O}$  enriched spectrum analyzed in Ref. [1] was a “side-product” of a large measurement campaign performed in 2018 at the AILES beam line of the SOLEIL synchrotron and dedicated to the characterization of the water vapor FIR absorption continuum by Fourier transform

spectroscopy (FTS) [2,3]. It turns out that, while we believed that the rotational spectrum involving the lowest vibrational states of water vapor was well characterized, some of the recorded SOLEIL high resolution spectra of  $^{18}\text{O}$  water vapor allowed for a substantial extension of the previous knowledge in the region, in addition to provide valuable tests of existing databases. This is mainly the result of the unique characteristics of the AILES beamline of the SOLEIL synchrotron light source in the “difficult” FIR spectral region where the performances of laboratory spectrometers are usually not optimum (see the review of various experimental approaches for FIR absorption spectroscopy in the introduction of Ref. [1]). The combination of the synchrotron radiation with a long path absorption cell allows for broad-band high sensitivity FIR recordings with a spectral resolution of about to  $0.001 \text{ cm}^{-1}$ . Note that in the case of the  $\text{H}_2^{18}\text{O}$  transitions assigned in [1], the weakest

\* Corresponding author.

E-mail address: [alain.campargue@univ-grenoble-alpes.fr](mailto:alain.campargue@univ-grenoble-alpes.fr) (A. Campargue).

**Table 1**

Experimental conditions of the five FTS spectra of natural water under analysis. The temperature was 295.5 K.

Sample	Pressure	Resolution, cm <sup>-1</sup>	Nb of scans
#1 Empty cell	≈ 1.7 μbar	0.001	320
Baseline	Pumping on the cell	0.05	200
#2 Sample	≈ 0.080 mbar	0.001	400
Baseline	Pumping on the cell	0.05	200
#3 Sample	≈ 0.91 mbar	0.001	480
Baseline	Pumping on the cell	0.05	200
#4 Sample	≈ 7 mbar	0.002	280
#5 Empty cell	≈ 0.15 μbar	0.001	220

measured lines have intensity on the order of  $10^{-25}$  cm/molecule which corresponds to a gain of 4 orders of magnitude of the detectivity threshold compared to previous H<sub>2</sub><sup>18</sup>O absorption measurements.

The importance of the FIR region in the Earth's radiation budget is a major motivation of the Far-infrared-Outgoing-Radiation Understanding and Monitoring (FORUM) mission of European Space Agency (<https://www.forum-ee9.eu/>). One of the identified goals of this mission is to “fill the observational gap across the far-infrared (from 100 to 667 cm<sup>-1</sup>), never before sounded in its entirety from space”. This requires an accurate knowledge of the water spectroscopy in the region and motivated us to apply for beam time at SOLEIL synchrotron for a new measurement campaign dedicated to the high resolution spectroscopy of various water isotopologues (natural, <sup>17</sup>O and D enriched) using the same experimental setup as for the <sup>18</sup>O enriched water recordings. The present contribution dedicated to the analysis and discussion of the natural water spectra recorded at five pressures up to 7 mbar, is the first one of the series.

The paper is organized as follows. In Section 2, we recall the experimental details including the spectrum acquisition, line list construction and spectra calibration. The main results are presented in Section 3 which presents an overview of the transitions contributing to the spectra together with a line position comparison with literature. In particular, we will consider (i) the HITRAN2020 spectroscopic database [4], (ii) the W2020 line lists of H<sub>2</sub><sup>16</sup>O, H<sub>2</sub><sup>18</sup>O and H<sub>2</sub><sup>17</sup>O with line positions computed from empirically determined energy levels [5] and, (iii) the calculations by Coudert et al. for the H<sub>2</sub><sup>16</sup>O main isotopologue using an effective Bending-Rotation Hamiltonian [6].

## 2. Experiment

### 2.1. Spectra acquisition

The FTS spectra were acquired on the AILES beam line of SOLEIL synchrotron facility operated in the 500 mA multibunch mode, in September 2021. A Bruker 125 interferometer with a 6 μm mylar-composite beam splitter and a 4 K cooled Si bolometer detector were used for the recordings. The absorption cell is a multipass cell in White-type configuration. The total absorption path length was set to 151.75 ± 1.5 m corresponding to 60 passes between mirrors separated by 2.52 m and about 0.5 m of space between the 50 μm thick polypropylene films windows. Five spectra were recorded for different pressure values up to 7 mbar, measured by a capacitance gage (Pfeiffer 10 mbar full range with corresponding accuracy of 0.01 mbar). The de-ionized water used for the recordings was frozen and liquefied several times before injection in the cell in order to minimize the presence of gas impurities. Table 1 summarizes the experimental conditions and the sequence of the recordings.

The first and last spectra were recorded at very low pressure, pumping on the cell in order to measure the strongest lines (in-

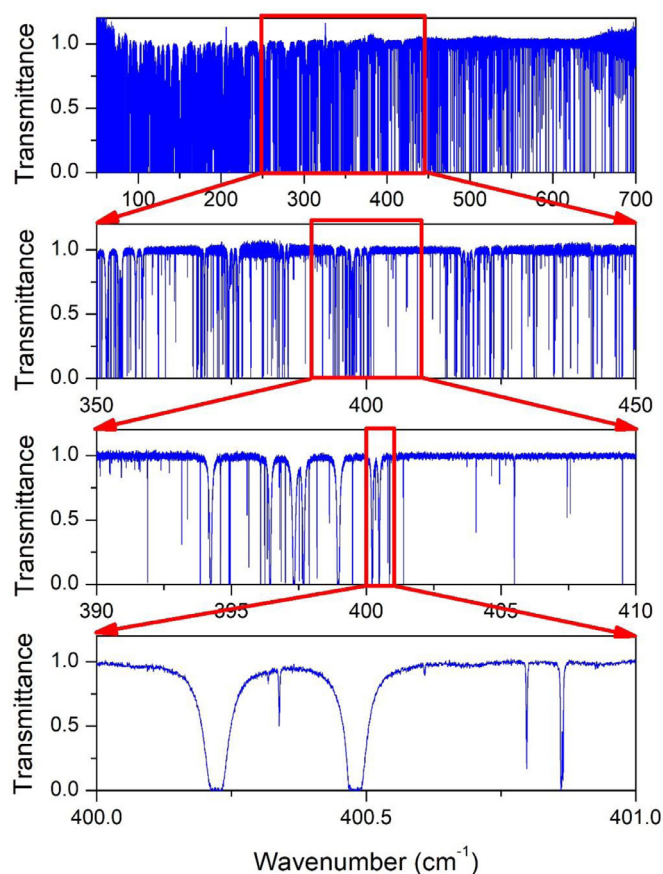


**Fig. 1.** Successive zooms of the FTS spectrum #3 of natural water vapor recorded at SOLEIL synchrotron at room temperature between 50 and 720 cm<sup>-1</sup> ( $P=0.91$  mbar).

tensity up to  $10^{-18}$  cm/molecule) and to check the stability of the frequency scale (see below). The other pressure values were set to about 0.085, 0.91 and 7.0 mbar. Except for the 7 mbar spectrum for which the pressure broadening allows for using a spectral resolution of 0.002 cm<sup>-1</sup>, the other spectra were recorded at the maximum spectral resolution of 0.00102 cm<sup>-1</sup> (defined as 0.9/MOPD where MOPD = 882 cm is the maximum optical path difference). No apodization of the interferogram was used (boxcar option of the Bruker software). The number of co-added spectra ranges between 200 and 480 (200 spectra corresponds to about 10 hours' acquisition at 0.001 cm<sup>-1</sup> spectral resolution or 5 h at 0.002 cm<sup>-1</sup> resolution). The baseline fluctuations were corrected prior to each high resolution recording. The temperature of 295.5(3) K was monitored by a pair of platinum sensors mounted on the cell external surface. An overview of the spectrum recorded at 0.91 mbar is displayed on Fig. 1, which includes successive zooms. The absorption coefficient was determined as  $\alpha_{total} = 1/L \ln(I_0(v)/I(v))$ , where  $L = 151.75$  m, and  $I(v)$  and  $I_0(v)$  correspond to the spectrum with the cell filled with water vapor and evacuated, respectively.

The observed line profiles result from different contributions. At 1 mbar, the pressure broadening (about  $4 \times 10^{-4}$  cm<sup>-1</sup> HWHM [4]) is equivalent to the width of the apparatus function (about  $3.5 \times 10^{-4}$  cm<sup>-1</sup> HWHM) while the Doppler broadening (proportional to the transition frequency) is on the order of  $1.5 \times 10^{-4}$  cm<sup>-1</sup> HWHM near 100 cm<sup>-1</sup>. The present study being mainly focused on line positions, each of the five transmittance spectra was fitted independently assuming the standard Voigt line profile as line shape (with adjusted Gaussian and Lorentzian widths) and no particular care was taken for the treatment of the apparatus function. The line parameters retrieval was performed

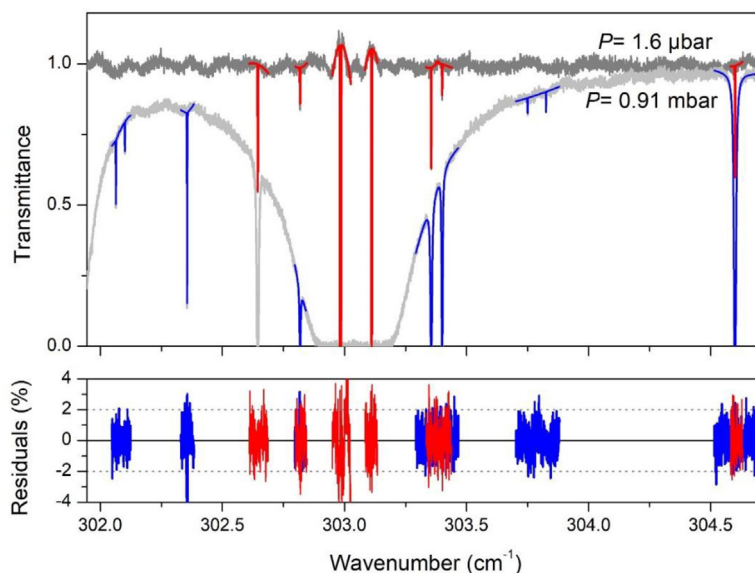


**Fig. 2.** Line parameter retrieval from the FTS spectra of water vapor near  $303\text{ cm}^{-1}$ . The line profile fit was performed in narrow spectral intervals around the lines which are not too saturated.

Upper panel: Recorded spectra #1 and #3 at  $\sim 1.6\text{ }\mu\text{bar}$  and  $0.91\text{ mbar}$ , respectively, (gray and light gray, respectively) with corresponding best fit spectra (red and blue, respectively).

Lower panel: Corresponding (exp. – fit) residuals in %.

using a homemade multiline fitting program in LabVIEW and C++. The HITRAN2020 line list was taken as starting point of the fit. For each spectrum, we selected a ten of isolated lines of intermediate intensity and adjusted their position, area, Gaussian and Lorentzian widths. The obtained Gaussian widths are larger than the Doppler broadening as they include an important contribution of the apparatus function. The average value of the fitted Gaussian widths was adopted as default value for all the fitted lines of a given spectrum. Fig. 2 illustrates the adopted procedure in a small spectral interval showing a very strong doublet (intensity larger than  $10^{-19}\text{ cm/molecule}$ ) near  $303\text{ cm}^{-1}$  for the spectra #1 (very low pressure) and #3 ( $0.91\text{ mbar}$ ). During the fit of the  $0.91\text{ mbar}$  spectrum, the doublet was omitted and line parameters of narrow lines were obtained from a local fit, even when these lines were located on the wing of the strong doublet. The line center of the two components of the doublet could be determined from a fit of the very low pressure spectrum (#1). The (exp. – calc.) residuals included in Fig. 2 are at the noise level ( $\sim 1\%$ ). This value corresponds to a noise equivalent absorption on the order of  $7 \times 10^{-7}\text{ cm}^{-1}$  and a detectivity threshold of about  $10^{-25}\text{ cm/molecule}$  for the line intensities measured in the  $0.91\text{ mbar}$  spectrum.

Overall, line parameters of 804, 1778, 1987, 1367 and 306 absorption features were retrieved for the spectra #1 to #5, respectively. In order to obtain a unique global line list, for each line, we selected the pressure condition of the best parameter determination of the considered line (intermediate transmittance value, limited overlapping with nearby lines) and kept the corresponding values for the global list. For a large fraction of lines, two spectra could be selected and the average line position and line intensity were adopted. In the list provided as Supplementary Material, the spectrum number (1 to 5, see Table 1) is attached to each line indicating the spectrum or spectra used for the retrieval. On the overview of the global list presented in the upper panel of Fig. 3, different colors are used according to the source of the line parameters.

During the data treatment, a number of lines were found in addition to those included in the HITRAN list of water vapor. They were identified as due to three impurity species:  $\text{CO}_2$ ,  $\text{NH}_3$  and  $\text{HF}$ . The  $\text{CO}_2$  lines are located in the high energy part of the recorded

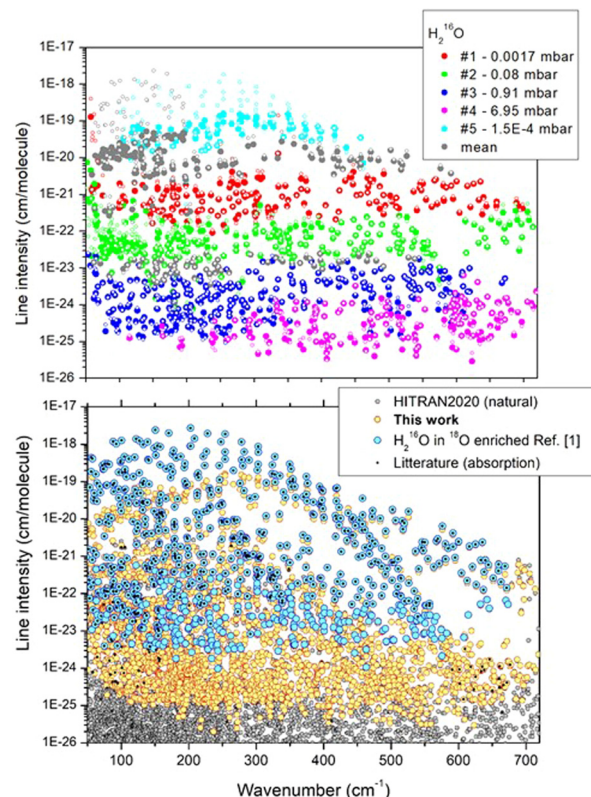


**Fig. 3.** Overview of different line lists for water vapor between  $40$  and  $720\text{ cm}^{-1}$ .

Upper panel: global line list constructed in this work from five spectra of natural water recorded at SOLEIL synchrotron at different pressures. Different colors are used for the spectrum chosen as source of the line parameters. Gray symbols mark the lines for which the position and intensity correspond to values averaged from two spectra. Small open circles correspond to the HITRAN list.

Lower panel: comparison of our global list (yellow dots) to (i) previous measurements available in the literature by absorption spectroscopy [7–20] (black dots), (ii)  $\text{H}_2^{16}\text{O}$  transitions identified in the spectrum of  $^{18}\text{O}$  enriched water recorded at SOLEIL synchrotron in [1] (blue dots), (iii) present recordings for natural water (yellow dots) and (iv) the HITRAN2020 line list [4] (gray dots).



region above  $640\text{ cm}^{-1}$  and belong to the  $\nu_2$  bending band. The relative abundance of  $\text{CO}_2$  was found to decrease sharply (from 5000 to 5 ppm) with the water vapor pressure indicating that it is due to a small leak or desorption. The HF and ammonia lines are rotational lines. Depending on the spectrum, about six HF lines are observed between 100 and  $350\text{ cm}^{-1}$  while ammonia lines are observed below  $200\text{ cm}^{-1}$ . Ammonia with a relative concentration of a few ppm is believed to be present as an impurity in the used water sample. HF is probably due to degassing from the O-ring seals of the cell.

After removal of the impurity lines and combination of the five datasets, the obtained global list includes 2867 water lines with intensities above  $2 \times 10^{-26}\text{ cm/molecule}$  (see overview in Fig. 3). Note that in the case of the spectra #1 and #5, the pressure was too small to be measured with the used pressure gage. Intensity comparison to the HITRAN values allowed to estimate the corresponding pressure values to about 1.7  $\mu\text{bar}$  and 0.15  $\mu\text{bar}$ , respectively. These pressure values were used in the calculation of the line intensities derived from these two spectra. As a result of the large pressure range of the recordings (from 0.15  $\mu\text{bar}$  to 7 mbar), the obtained experimental list includes line intensities spanning six orders of magnitude.

## 2.2. Frequency calibration

Before combining the five line lists into a single global list, we checked that no significant variation of the frequency calibration of the different spectra was observable: the position differences compared to HITRAN were found independent on the spectrum (see left panel of Fig. 4). The absolute frequency calibration was performed considering line positions provided in the HITRAN database with an uncertainty better than  $10^{-5}\text{ cm}^{-1}$ . A total of about 700 isolated lines with good signal-to-noise ratio were selected in the different recorded spectra and matched to the HITRAN reference lines. Note that the 7 mbar spectrum for which

pressure shifts on the line positions might be significant was excluded. According to Refs. [21–27], the self-pressure shifts for rotational lines are between  $-0.058$  and  $+0.045\text{ cm}^{-1}/\text{atm}$ . So, it means that at the maximum pressure of 7 mbar of our measurements, the line shifts can reach  $\pm 4 \times 10^{-4}\text{ cm}^{-1}$ , a value larger than the precision of the line center determination in the 7 mbar spectrum. The differences between the experimental line centers and the HITRAN values were globally linearly fitted. Excluding a ten of outliers, an *rms* deviation of  $2.42 \times 10^{-5}\text{ cm}^{-1}$  was obtained for the linear fit, thus larger than the accuracy of the position of the reference lines. The obtained empirical correction of the frequencies  $[+8.4(6) \times 10^{-5} - 6.30(7) \times 10^{-7} \sigma]$ , where  $\sigma$  is the measured wavenumber in  $\text{cm}^{-1}$  was applied to all the positions of the global list. A value of  $5 \times 10^{-5}\text{ cm}^{-1}$  seems to be a reasonable estimate for the resulting uncertainty on the experimental position values of the “good” lines (isolated unsaturated lines measured in the low pressure spectra). In the global line list provided as Supplementary Material, the fit error on the line position determination is included. For a significant fraction of the lines, the fit uncertainty (thus excluding the frequency calibration error) was found smaller than  $5 \times 10^{-5}\text{ cm}^{-1}$  and is thus believed to largely underestimate the real uncertainty on the line position. For all these lines, we replaced the fit uncertainty by a value of  $5 \times 10^{-5}\text{ cm}^{-1}$ . Note that the uncertainty of the weakest or highly blended lines can reach a value of  $1 \times 10^{-3}\text{ cm}^{-1}$  in the worst cases.

The histogram of the position differences is presented Fig. 4 for the lines used for the frequency calibration and for the whole set of measurements. A significant fraction of the measured lines shows position differences larger than our experimental error bar. In the following, we will examine these lines in order to determine the reasons for these discrepancies.

As concerns line intensities, we do not claim for a high accuracy of the reported values. The limited number of points describing the line profile and the impact of the apparatus function which was roughly taken into account in the line parameter retrieval limit

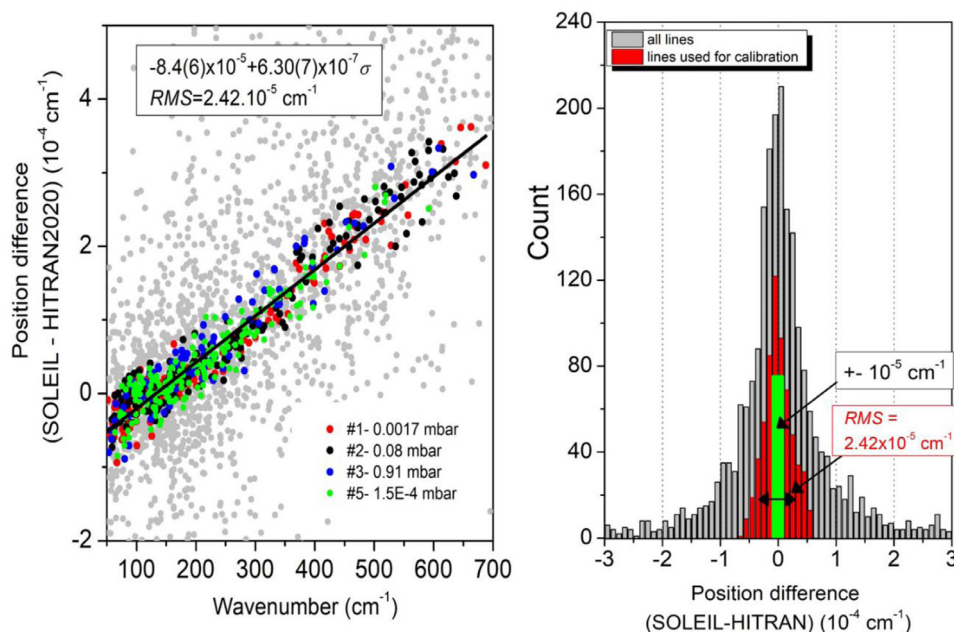


**Fig. 4.** Frequency calibration of the FTS spectra of natural water recorded at SOLEIL synchrotron.

*Left panel:* The colored symbols correspond to the differences between the line centers retrieved from the different recorded spectra and reference line positions provided with an uncertainty better than  $10^{-5}\text{ cm}^{-1}$  in the HITRAN database [4]. The 7 mbar spectrum for which pressure shifts on the line positions might be significant is excluded. The global dataset was fitted by a linear function providing the frequency correction to be applied to the measurements. Gray symbols correspond to the comparison to all the HITRAN line positions (*rms* deviation of  $2.42 \times 10^{-5}\text{ cm}^{-1}$ ).

*Right panel:* Histograms of the (meas. - HITRAN) position differences for the lines used for the frequency calibration (red) and for the whole set of measurements. The green bars correspond to the HITRAN uncertainty of the used reference lines ( $\pm 10^{-5}\text{ cm}^{-1}$ ).

**Table 2**

Statistics of the rovibrational assignments of the five spectra of natural water recorded at SOLEIL at various pressures up to 7 mbar.

Molecule	NT <sup>a</sup>	NT <sub>new</sub> <sup>b</sup>	J	K <sub>a</sub>	Range, cm <sup>-1</sup>
H <sub>2</sub> <sup>16</sup> O	1310	96 (385)	22	14	51.43 – 718.43
H <sub>2</sub> <sup>18</sup> O	564	3 (3)	18	12	53.57 – 702.59
H <sub>2</sub> <sup>17</sup> O	407	3 (3)	17	10	53.51 – 694.38
HD <sup>16</sup> O	674	46 (63)	19	12	50.27 – 591.88
HD <sup>18</sup> O	42		10	7	78.51 – 310.10
HD <sup>17</sup> O	4		6	4	168.17 – 255.19
Total	3001	148 (454)	22	14	50.27 – 718.43

Notes:

<sup>a</sup> Number of assigned transitions.<sup>b</sup> Number of newly observed transitions. The first number considers previous studies by absorption and emission. The number between parenthesis considers only absorption studies.

the accuracy of the retrieved values. The fit uncertainty included in the global line list is only indicative. Comparisons to HITRAN intensity values indicate that, excluding the two lowest pressure spectra (#1 and #5), most of the line intensities agree with HITRAN values within  $\pm 10\%$ . The comparison of the fitted intensities to HITRAN values shows deviations largely exceeding the fit uncertainty. Relying on HITRAN values, we conclude that the fit error of our experimental intensities is probably underestimated for a small fraction of the measurements. Our accuracy was nevertheless sufficient to evidence a clear HDO enrichment in the spectra, probably due to a previous contamination by deuterated species adsorbed on the cell walls. Compared to the natural abundance, the enrichment was larger by about a factor of two for the first recorded spectra and then, as a consequence of the successive fillings and evacuations of the cell, gradually decreased to reach practically the natural value for the last recording. In the case of the most intense lines which were retrieved from spectra #1 and #5 (intensity up to  $10^{-18}$  cm/molecule), saturation effects are considerable and the fitted values of the intensities are strongly underestimated by a factor up to 10 in the worst cases (see Fig. 3).

### 3. Analysis and comparison with literature

The HITRAN2020 rovibrational assignments of practically all observed water transitions have been validated and transferred to our list. The HITRAN rovibrational assignment of five high  $J$  transitions in the pure rotational band of H<sub>2</sub><sup>17</sup>O (taken from Lodi and Tennyson [28]) is incomplete in the HITRAN list [4]. The complete assignment is provided in our list. Overall, the 2867 measured water lines were assigned to 3001 transitions of six isotopologues (H<sub>2</sub><sup>16</sup>O, H<sub>2</sub><sup>18</sup>O, H<sub>2</sub><sup>17</sup>O, HD<sup>16</sup>O, HD<sup>18</sup>O, and HD<sup>17</sup>O). Table 2 presents some global characteristics of the assigned transitions, including the maximum values of the  $J$  and  $K_a$  rotation quantum numbers and the numbers of transitions firstly observed compared to previous absorption studies available in the literature. Overall 454 transitions are newly observed. The list of these newly observed lines is provided as a second Supplementary Material. Part of these lines (306) was previously observed by emission spectroscopy (mostly in [19] and [29] – see below). The line position comparison to the most relevant emission study is included the Supplementary Material.

#### 3.1. Overview of previous experimental studies in the region

The review of previous works on the rotation and vibration-rotation transitions of water in our region includes studies by absorption [7–20] and by emission spectroscopy in flames or discharges [6,19,29–34]. Overall, 686 H<sub>2</sub><sup>16</sup>O rotational transitions were recorded in absorption [7–20] for the five lowest states – (000),

(010), (020), (001), and (100) – up to a maximum value of the rotation quantum number  $J_{\max} = 17$ . About 240 transitions were newly measured by absorption in Ref. [1], leaving 375 new observations for the present study. More than 6000 transitions involving 14 vibration states were assigned in emission spectra in our region [6,19,29–33]. The maximum value of the rotational quantum number in the ground state (000) is  $J_{\max} = 41$  [33]. The overall position accuracy of emission studies is generally worse than the present accuracy. The most precise set of line positions reported by emission spectroscopy [6,19,29] have an accuracy of  $4.0 \times 10^{-4}$  cm<sup>-1</sup> at best.

In the spectrum of water vapor highly enriched in <sup>18</sup>O recorded at SOLEIL synchrotron with the same setup as the one used for the present recordings, 37 additional H<sub>2</sub><sup>16</sup>O transitions up to  $J_{\max} = 19$  were reported [1]. Compared to this study, the average value of the position differences is  $3.44 \times 10^{-5}$  cm<sup>-1</sup> with an *rms* deviation of  $13.37 \times 10^{-5}$  cm<sup>-1</sup> for 604 transitions in common in the two studies. Taken into account that the H<sub>2</sub><sup>16</sup>O relative abundance was only 5% in the spectrum analyzed in Ref. [1], the achieved agreement is very satisfactory and illustrates the consistency of the independent frequency calibration of the two spectra.

The observations relative to the H<sub>2</sub><sup>18</sup>O minor isotopologue are more limited. Overall, 525 (mainly pure rotation) transitions were reported in seven absorption [7,9,13,34–37] and one emission [38] studies. Only six rotation transitions for the (010), (020) and (100) states were measured in these previous studies [9,34]. The most extended H<sub>2</sub><sup>18</sup>O line list (more than 730 transitions) was obtained from the SOLEIL spectrum analyzed in Ref. [1]. It includes more than 300 transitions of the (010) – (010) and (020) – (020) bands. The comparison of our H<sub>2</sub><sup>18</sup>O line positions shows a very good agreement to the highly precise data of Matsushima et al. [37]. The *rms* deviation is  $6.19 \times 10^{-5}$  cm<sup>-1</sup> for 98 transitions observed in both measurements.

For H<sub>2</sub><sup>17</sup>O, 362 pure rotation transitions were reported by absorption in Refs. [7,13,35–37]. The list of H<sub>2</sub><sup>17</sup>O rotation transitions was extended up to 685 in Ref. [1], including 114 transitions of the (010) – (010) band. Now, we are reporting 407 transitions (see Table 2). A very good agreement is obtained with the highly precise positions of Matsushima et al. [37]. The *rms* deviation is  $4.02 \times 10^{-5}$  cm<sup>-1</sup> for 103 transitions observed in both measurements. The comparison with our previous measurement [1] gives an *rms* deviation of  $2.93 \times 10^{-4}$  cm<sup>-1</sup> for 345 transitions with position discrepancies greater than 0.001 cm<sup>-1</sup> for weak component of unresolved pure rotational doublet  $17_{117} - 16_{016}$  at 319.6949 cm<sup>-1</sup> and strongly blended components of the doublet  $6_{61} - 5_{50}$  and  $6_{60} - 5_{51}$  at 301.142 cm<sup>-1</sup>.

In the case of HD<sup>16</sup>O, 510 absorption and 1422 emission transitions were reported in Refs. [7,9,10,39,40]. In addition, 133 previously unobserved transitions were reported in Ref. [1]. 674 HD<sup>16</sup>O transitions were measured in the present work, 63 of which being firstly detected in absorption. The best position agreement is obtained for Refs. [1,9,10] with corresponding *rms* values of  $1.49 \times 10^{-4}$ ,  $2.78 \times 10^{-4}$  and  $1.74 \times 10^{-4}$  cm<sup>-1</sup> for 488, 204 and 267 transitions respectively. The comparison to the less accurate data of Refs. [7,40] leads to *rms* values of  $3.22 \times 10^{-3}$  and  $3.66 \times 10^{-3}$  cm<sup>-1</sup> for 60 and 55 transitions, respectively. The maximum deviation reaches a value of 0.0138 cm<sup>-1</sup> for the absorption study of Ref. [7] and 0.0169 cm<sup>-1</sup> for the emission study of Ref. [40].

For HD<sup>18</sup>O, the first measurements were due to Johns [9] who reported 148 pure rotation transitions between 78 and 220 cm<sup>-1</sup>. In our recent study [1], we extended the observations to 1126 transitions in the range 44.86 – 645.74 cm<sup>-1</sup>. All 42 transitions reported in the present work were observed in Ref. [1]. Note that some of the present line positions are nevertheless believed to be more precise because the corresponding lines were saturated in Ref. [1].

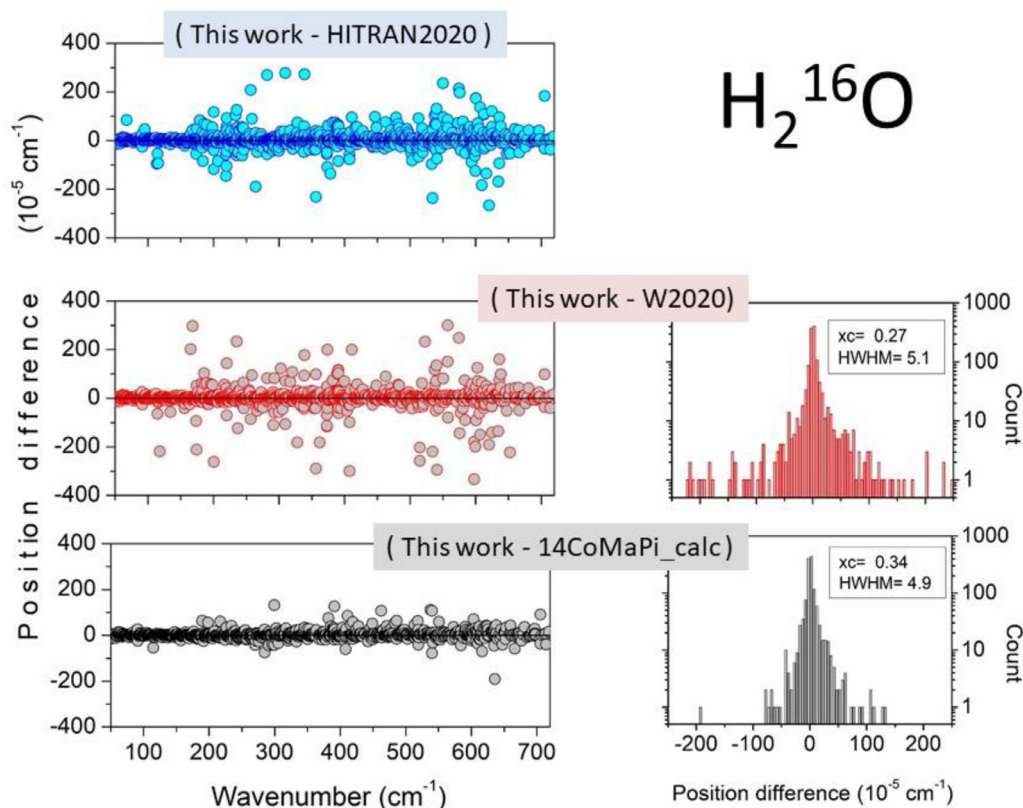


**Fig. 5.** Position comparison of the  $\text{H}_2^{16}\text{O}$  lines in the 50–720  $\text{cm}^{-1}$  range.

*Left panels:* Differences between the experimental values presently determined from SOLEIL spectra to the HITRAN2020 data, to the W2020 empirical values and the values calculated using a rotation-bending Hamiltonian [6] (14CoMaPi).

*Right panels:* Histograms of the deviations between the experiment and the W2020 and 14CoMaPi positions. The center (xc) and HWHM obtained from a Gaussian fit of the histograms are given on the plot (in  $10^{-5} \text{ cm}^{-1}$  units).

The line position comparison with data of Johns [9] leads to an *rms* deviation of  $3.66 \times 10^{-4} \text{ cm}^{-1}$  for 26 transitions.

### 3.2. Validation tests of the HITRAN2020, W2020 and 14CoMaPi line positions

Let us now compare our results to the most relevant spectroscopic databases in our region.

Following the approach developed by a task group (TG) of the International Union of Pure and Applied Chemistry (IUPAC-TG) [41–44], improved sets of empirical energy levels have been recently released for  $\text{H}_2^{16}\text{O}$ ,  $\text{H}_2^{18}\text{O}$  and  $\text{H}_2^{17}\text{O}$ . The W2020 empirical energy levels of Ref. [5] were derived from an exhaustive collection and review of measured transitions in all spectral regions [5,45]. The procedure and code xMARVEL [46,47] were applied to the constructed catalog of measured absorption and emission line positions. In particular, all the above reviewed sources of measurements in the rotational region of interest were incorporated in the transition datasets. In the present work, no new energy levels could be determined from the recorded spectra *i.e.* all the energy levels involved in the transitions presently measured have an empirically determined W2020 value (tag “M” in the W2020 lists [5]). An important advantage of the Ritz principle which is the basis of the MARVEL procedure is that it allows to obtain line positions with experimental accuracy even for transitions which were not previously measured. Direct validation tests when experimental spectra become available are nevertheless suitable (see *e.g.* Refs. [48–50]). The transitions newly observed in the present SOLEIL spectra are particularly valuable in that context. Let us underline that the rotational region under analysis is of importance as a large

fraction of the involved energy levels are lower state of transitions located in the whole frequency range of the water absorption spectrum. Errors or inaccuracies evidenced in the rotational region may impact line positions calculated from empirical energy values in the entire water spectrum.

As mentioned above, according to the HITRAN2020 source list, most of the HITRAN position values should coincide to the W2020 empirical positions of Ref. [5]. In fact, as already discussed in Ref. [50] and illustrated below, this is not the case. The origin of this situation remains unclear and might possibly lead to an update of the HITRAN2020 list. Thus separated comparison has to be performed to the HITRAN and W2020 line lists.

The bending-rotation Hamiltonian developed by Coudert et al. [6] (14CoMiPa, hereafter) provides an alternative source of calculated line positions in our region for the main isotopologue. Due to the failure of the approach based on a rotational Hamiltonian of a semi-rigid molecule in the case of water, a bending rotation Hamiltonian has been developed to account for the  $\text{H}_2^{16}\text{O}$  spectrum up to the second triad and to  $J=30$  [6]. The effective Hamiltonian parameters were determined from a weighted least-squares fitting of a large set of 24,461 literature data including rotational energy levels, microwave, far infrared, and infrared measured transition frequencies.

We present in Fig. 5 an overview comparison of our line positions of the main isotopologue to the values included in the HITRAN database, to the W2020 values [5] and to the calculated values of Coudert et al. [6]. The corresponding comparison table is provided as a third Supplementary Material. Fig. 5 illustrates that the overall agreement between the experiment and the three databases is excellent. For instance, the histograms of the W2020



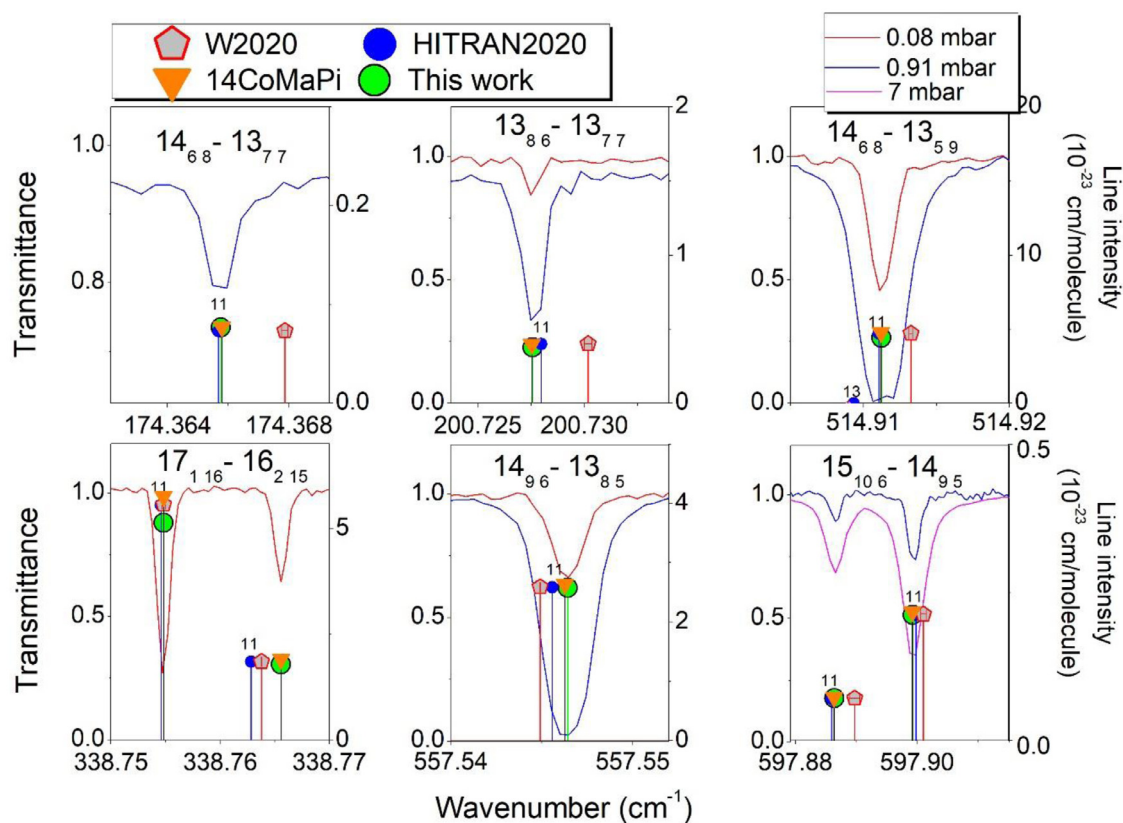


**Fig. 6.** Comparison of FTS spectra of natural water vapor recorded at SOLEIL and corresponding global line list constructed in this work (green circles) to the W2020 list of H<sub>2</sub><sup>16</sup>O [5] (red pentagons). The HITRAN2020 stick spectrum of natural water (blue circles) is superimposed together with the effective Hamiltonian calculated positions of Ref. [6] (orange triangles - 14CoMaPi). All the displayed examples correspond to inaccuracies of the HITRAN2020 positions of the H<sub>2</sub><sup>16</sup>O main isotopologue (isotopologue code "11"). All the problematic lines correspond pure rotational transitions. Their rotational assignments are given on each panel.

and 14CoMaPi deviations from experiment show a similar Gaussian distribution centered at about of  $3 \times 10^{-6} \text{ cm}^{-1}$  for 1310 transitions with a HWHM of  $5 \times 10^{-5} \text{ cm}^{-1}$ , corresponding to our claimed position uncertainty of the "good" lines. The most noticeable differences between the three comparisons is the presence of some relatively large deviations for the W2020 and HITRAN2020 data while these "outliers" are mostly absent for 14CoMaPi. At this point, it is worth mentioning that the comparison applies to the same set of 1310 transitions as all our H<sub>2</sub><sup>16</sup>O observations have a counterpart in the three databases (except for a couple of doublets missing in the HITRAN database – see below).

The direct comparison to the spectra presented in Figs. 6 and 7 gives insights on the significance of these outliers. Fig. 6 shows six examples for which clear deviations are observed for the W2020 line positions of Ref. [5] while HITRAN position (given with W2020 source!!) agree with the measurements. The W2020 position uncertainties (displayed on the figure) are significantly smaller than the observed deviations. For instance, for the lines displayed at 338.7656 and 557.5464 cm<sup>-1</sup>, the (exp. - W2020) position differences are  $1.77 \times 10^{-3}$  and  $1.51 \times 10^{-3} \text{ cm}^{-1}$ , respectively, 74 and 101 times larger than the claimed W2020 uncertainties ( $2.4 \times 10^{-5}$  and  $1.5 \times 10^{-5} \text{ cm}^{-1}$ , respectively [5]).

In Fig. 7, we present six examples of H<sub>2</sub><sup>16</sup>O transitions where neither the W2020 position nor the HITRAN position shows a satisfactory agreement with experiment. All these lines are supposed to have a W2020 source in the HITRAN2020 database.

The H<sub>2</sub><sup>16</sup>O calculated stick spectrum of 14CoMaPi [6] is included in the different panels of Figs. 6 and 7. In all the displayed examples, the 14CoMaPi line positions agree with experiment. This observation nicely illustrates the fact that the physics included in

the bending-rotation Hamiltonian of Ref. [33] brings constraints which improves the accuracy of the calculations beyond the experimental accuracy of the input data. Although the accuracy of the previous frequency measurements of the transitions observed in the SOLEIL spectra was not optimum, the fit of the effective Hamiltonian parameters benefitted from a large set of spectroscopic data extending beyond our spectral range. It is important to note that all the experimental sources used by Coudert et al. [6] in 2014 are publicly available and were used for the derivation of the W2020 energy levels. The absence of "outliers" in the 14CoMaPi list suggests that for our set of observations in the rotational range, the effective Hamiltonian approach is more efficient to avoid "outliers" than the xMARVEL approach [46,47] implemented to derive the W2020 energy levels [5,45].

In principle, the W2020 empirical energy levels and transition frequencies also benefitted from experimental sources in other spectral regions which should improve their accuracies but the constraints brought by the large networks connecting the energy levels are different compared to those brought by the effective Hamiltonian of Ref. [6]. As a result, some individual energy levels can be strongly impacted by an experimental source reporting an inaccurate measurement and the resulting W2020 transitions frequency is inaccurate. In three previous contributions by cavity ring-down spectroscopy (CRDS), we presented validation tests of the W2020 positions. In the 8040–8630 cm<sup>-1</sup> region and in the region of the A-band of O<sub>2</sub> near 760 nm [48–50], a significant number of substantial deviations of the W2020 positions from the measurements were evidenced. Part of the W2020 positions were found less accurate than some original sources included in the W2020 transition database and W2020 uncertainties were found

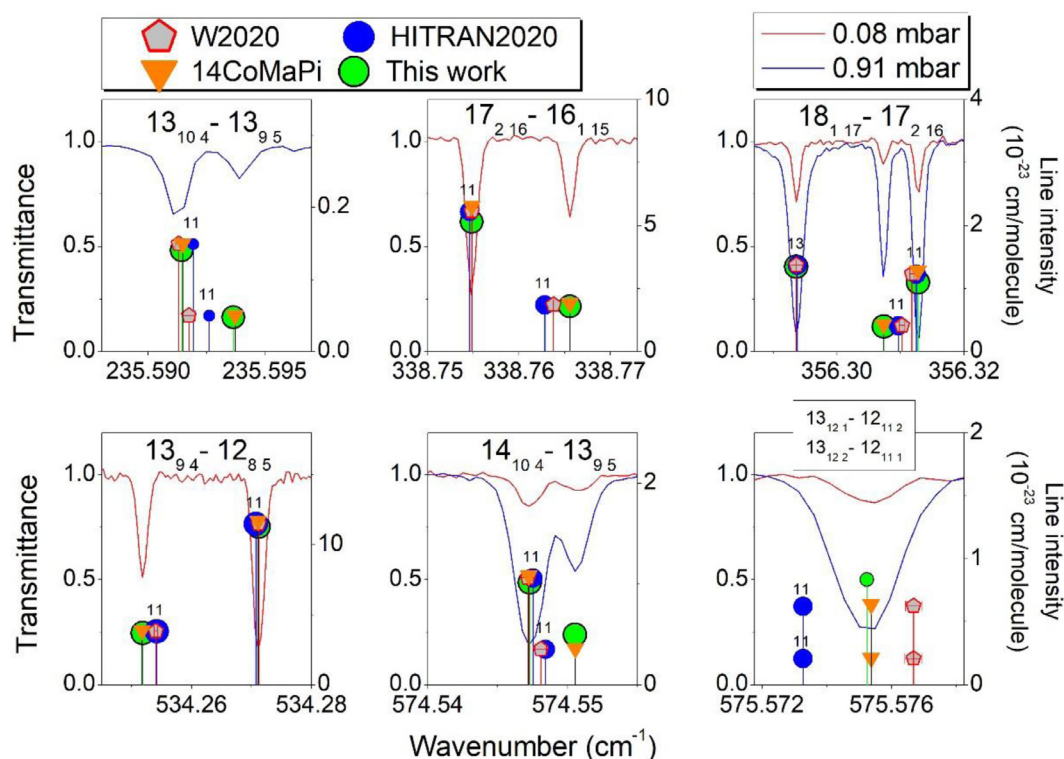


**Fig. 7.** Examples of inaccurate line positions in both the W2020 and HITRAN2020 lists. Comparison of FTS spectra of natural water vapor recorded at SOLEIL and corresponding global line list constructed in this work (green circles) to the W2020 list of  $\text{H}_2^{16}\text{O}$  [5] (red pentagons) and to the  $\text{H}_2^{16}\text{O}$  calculated positions of Ref. [33] (orange triangles - 14CoMaPi). All the displayed examples correspond to inaccuracies of both the W2020 and HITRAN2020 positions of the  $\text{H}_2^{16}\text{O}$  main isotopologue (isotopologue code "11"). All the problematic lines correspond pure rotational transitions. Their rotational assignments are given on each panel.

unreliable. In particular, at high energy, a significant fraction of the W2020 position were found to deviate from observations by amounts exceeding their claimed uncertainty by factors  $>10$ – $100$  [49,50]. They are due to the fact that the authors of Ref. [5] used not only high-precision data to determine the W2020 energies and some less accurate data are ‘spoiling’ higher quality data sources. For instance, a large number of transitions from emission spectra [30–33,51–58], including very old data [59–61] were incorporated in the xMARVEL procedure [5,45]. As a result, the few high-precision data did not have a decisive influence on the determination of the corresponding W2020 energies. For example, the very accurate line positions [1] of the pure rotation transitions  $17_2 16 - 16_1 15$  ( $338.76545 \text{ cm}^{-1}$ , [1]) and  $18_1 17 - 17_2 16$  ( $356.30704 \text{ cm}^{-1}$ , [1]) were included in the input data file of Refs. [5,46] but the resulting W2020 values reported with error bars of  $2.4 \times 10^{-5}$  and  $4.6 \times 10^{-4} \text{ cm}^{-1}$  deviate by  $-1.67 \times 10^{-3} \text{ cm}^{-1}$  and  $+3.21 \times 10^{-3} \text{ cm}^{-1}$ , respectively. The position values of Ref. [1] are confirmed by the present measurements (average differences of  $1.0 \times 10^{-4} \text{ cm}^{-1}$  and  $3.1 \times 10^{-4} \text{ cm}^{-1}$ , respectively).

In a fourth Supplementary Material, we provide a table limited to the lines of the global line list whose measured position differs from the W2020 value by more than  $9 \times 10^{-4} \text{ cm}^{-1}$ . A sample of the table is presented in Fig. 8. The ratio  $R = \frac{|v_{\text{exp}} - v_{\text{W2020}}|}{\Delta v_{\text{W2020}}}$  which compares the absolute deviation of the W2020 position from the measured value to the claimed W2020 position uncertainty has been added. Over the 60 listed transitions, all but two have an  $R$  value larger than unity and 21 correspond to  $R > 10$  (with maximum value  $R = 459$  for pure rotational transition  $15_5 11 - 14_4 10$  at  $388.70559 \text{ cm}^{-1}$ ), illustrating the limited reliability of the W2020 uncertainties for the considered set of lines. The (exp-14CoMaPi\_calc) position differences are included

in the table. For 45 of the 60 transitions listed, the deviation from the 14CoMaPi calculated value is less than  $2 \times 10^{-4} \text{ cm}^{-1}$ . Only three (exp-14CoMaPi) deviations exceeding  $9 \times 10^{-4} \text{ cm}^{-1}$  are noted. They correspond to very weak lines (line intensity smaller than  $1.6 \times 10^{-25} \text{ cm/molecule}$ ) and have probably an experimental origin.

As concerns the HITRAN database, except for two  $J' = 21$  doublets, the source given for the  $\text{H}_2^{16}\text{O}$  line positions is the W2020 line list [5]. Even if the position values are not exactly the original values published by Furtenbacher et al. [5] (see for instance the upper panels of Fig. 6), the presence of outliers in the HITRAN list has the W2020 origin discussed above. For the  $(21_0 21 - 20_1 20)$  and  $(21_1 21 - 20_0 20)$  and  $(21_1 20 - 20_2 19)$  and  $(21_2 20 - 20_1 19)$  doublets, the HITRAN database reproduces the values of Lanquetin et al. [62] (thus obtained following the same approach as adopted in 14CoMaPi). The comparison to experiment indicates that this choice was judicious as for instance, the measured position of the first doublet is closer to the value of Lanquetin et al. [62] than to the W2020 value ( $6.4 \times 10^{-4} \text{ cm}^{-1}$  and  $1.1 \times 10^{-3} \text{ cm}^{-1}$  position differences, respectively).

The pure rotation  $\text{H}_2^{16}\text{O}$  doublet,  $22_1 22 - 21_0 21$  and  $22_0 22 - 21_1 21$ , assigned to the line measured at  $407.74639 \text{ cm}^{-1}$  (intensity of  $1.313 \times 10^{-25} \text{ cm/molecule}$ ) is the only observed line absent in the HITRAN2020 list. The W2020 positions and intensities [5] agree satisfactorily with the measurements ( $407.74939 \text{ cm}^{-1}$  and  $1.04 \times 10^{-25} \text{ cm/molecule}$ , respectively). Let us now consider the minor isotopologues

The W2020 transition frequencies have been published only for the non-deuterated species ( $\text{H}_2^{16}\text{O}$ ,  $\text{H}_2^{18}\text{O}$ ,  $\text{H}_2^{17}\text{O}$ ) [5]. In the case of the deuterated species –  $\text{HD}^{16}\text{O}$ ,  $\text{HD}^{18}\text{O}$ , and  $\text{HD}^{17}\text{O}$  –, the HITRAN database reproduces the line positions calculated by



HITRAN2020											W2020													
spc	Nu_exp	dN	S_exp	dS	Nu	S	assignment				d1	Ratio_1	Nu	t	dN1	S	d2	Ratio_2	R	d3				
3	118.04454	5	1.869E-24	6	118.044535	1.997E-24	000	14	6	8	000	14	5	9	1	0.936	118.04673	M	4	2.002E-24	-219	0.934	54.8	-9
3	165.07328	5	1.435E-24	3	165.073002	1.598E-24	000	14	7	7	000	14	6	8	28	0.898	165.07126	M	35	1.601E-24	202	0.896	5.8	1
3	168.09872	11	2.589E-25	11	168.098288	2.399E-25	000	15	5	11	000	14	6	8	43	1.079	168.09575	M	16	2.405E-25	297	1.077	18.6	-8
3	173.65217	8	8.392E-25	8	173.652719	8.024E-25	000	15	6	10	000	15	5	11	-55	1.046	173.65311	M	20	8.044E-25	-94	1.043	4.7	1
3	174.36575	5	7.695E-25	4	174.365673	7.317E-25	000	14	6	8	000	13	7	7	8	1.042	174.36787	M	11	7.338E-25	-212	1.049	19.3	-3
3	185.67453	5	1.807E-24	3	185.673836	1.911E-24	000	15	5	11	000	15	4	12	69	0.946	185.67350	M	14	1.916E-24	103	0.943	7.4	-2
3	200.72759	5	3.778E-24	5	200.727999	4.003E-24	000	13	8	6	000	13	7	7	-41	0.944	200.73021	M	17	4.013E-24	-262	0.941	15.4	3
3	220.52085	5	1.150E-24	3	220.519932	1.041E-24	000	14	9	6	000	14	8	7	92	1.105	220.51942	M	6	1.043E-24	143	1.103	23.8	4
3	235.59390	5	4.761E-25	7	235.592641	4.969E-25	000	13	10	4	000	13	9	5	126	0.958	235.59157	M	33	4.983E-25	233	0.955	7.1	-9
3	236.92234	7	3.869E-25	6	236.922838	3.507E-25	000	14	10	5	000	14	9	6	-50	1.103	236.92358	M	35	3.516E-25	-124	1.100	3.5	0
3	258.66921	5	3.136E-24	3	258.668316	3.176E-24	000	16	2	14	000	16	1	15	89	0.987	258.66827	M	14	3.184E-24	94	0.985	6.7	5
2	291.44779	5	2.479E-23	3	291.448007	2.408E-23	000	16	2	15	000	16	1	16	-22	1.029	291.44889	M	8	2.415E-23	-110	1.027	13.8	10
1	302.64445	5	1.114E-21	3	302.644081	9.033E-22	000	16	1	16	000	15	0	15	37	0.925	302.64323	M	3	9.059E-22	122	0.922	40.7	-16
3	309.78911	5	5.228E-24	3	309.789058	5.544E-24	000	17	1	16	000	17	0	17	5	0.943	309.79017	M	8	5.560E-24	-106	0.940	13.3	14

**Fig. 8.** Beginning of a Table provided as a Supplementary Material listing the absorption lines extracted from the global line list of water vapor between 50 and 720  $\text{cm}^{-1}$  whose measured position differs from the W2020 position by more than  $0.0009 \text{ cm}^{-1}$ . The (exp-HITRAN2020), (exp-W2020) and (exp-14CoMaPi) position differences are given in  $10^{-5} \text{ cm}^{-1}$  units in columns, d1, d2 and d3, respectively. The ratio  $R = |d2|/dN1$  compares the absolute deviation of the W2020 position to the W2020 position uncertainty (dN1).

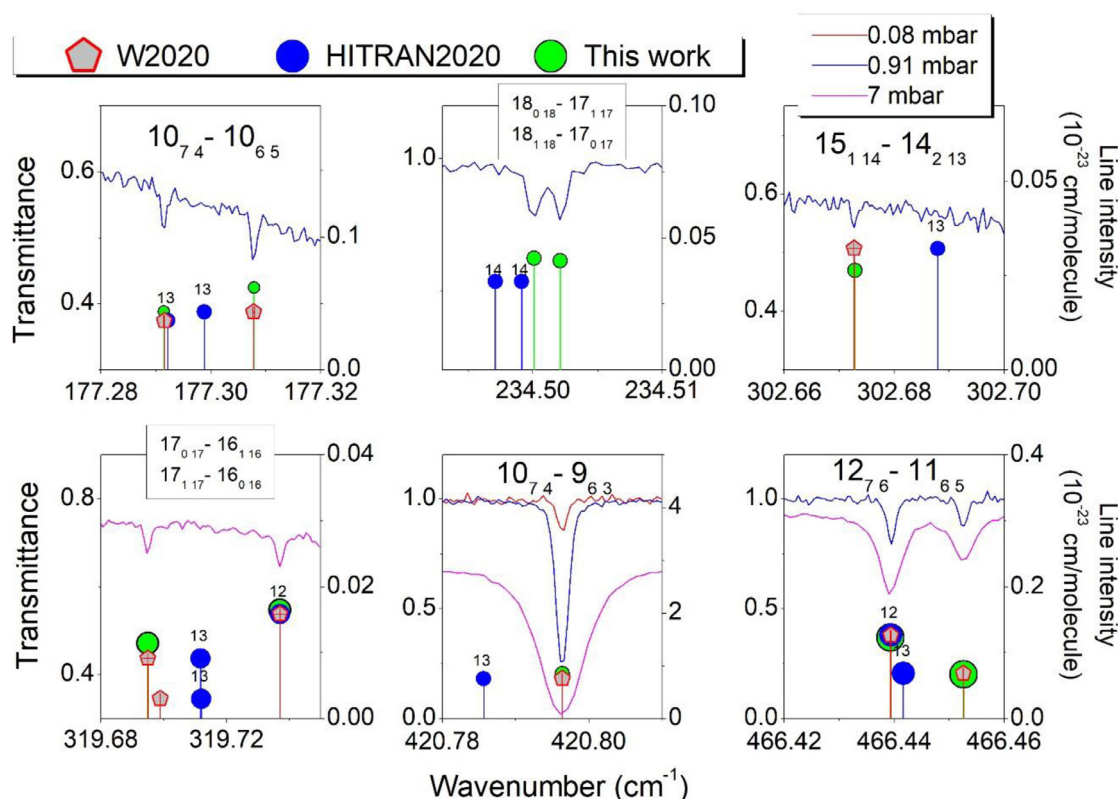


**Fig. 9.** Examples of inaccurate line positions in the HITRAN database. Comparison of FTS spectra of natural water vapor recorded at SOLEIL and corresponding global line list constructed in this work (green circles) to the HITRAN2020 list of natural water [4] (blue circles). All but the  $\text{HD}^{16}\text{O}$  doublet (isotopologue code “14”) near  $234.50 \text{ cm}^{-1}$  are relative to the  $\text{H}_2^{17}\text{O}$  minor isotopologue (isotopologue code “13”). The W2020 line list of  $\text{H}_2^{17}\text{O}$  [5] is superimposed (red pentagons) with corresponding error bars. In all the displayed examples, the W2020 line positions are in good agreement with experiment. All the problematic lines correspond pure rotational transitions. Their rotational assignments are given on each panel.

Kyuberis et al. [63] from updated IUPAC-TG energy levels [42]. The general agreement is satisfactory for the line positions of deuterated species. The *rms* deviations of our line positions from those of HITRAN [4] are  $3.74 \times 10^{-4}$ ,  $6.62 \times 10^{-4}$  and  $4.54 \times 10^{-4} \text{ cm}^{-1}$  for 674, 42 and 4 transitions of  $\text{HD}^{16}\text{O}$ ,  $\text{HD}^{18}\text{O}$  and  $\text{HD}^{17}\text{O}$  respectively. Nevertheless, the line position differences exceed  $0.001 \text{ cm}^{-1}$  for twelve  $\text{HD}^{16}\text{O}$  and one  $\text{HD}^{18}\text{O}$  transitions. The maximum deviations are for high  $J$ ,  $K_a$  transitions of  $\text{HD}^{16}\text{O}$  (up to  $0.0043 \text{ cm}^{-1}$ ) and for the  $2_{20} - 1_{11}$   $\text{HD}^{18}\text{O}$  transition ( $0.0042 \text{ cm}^{-1}$ ). Note, the *rms* deviation for 41 transitions of  $\text{HD}^{18}\text{O}$  (excluding the  $2_{20} - 1_{11}$  transition) is  $1.26 \times 10^{-4} \text{ cm}^{-1}$ .

For the  $\text{H}_2^{18}\text{O}$  species, again we noted some differences between HITRAN2020 and W2020 line positions while the HITRAN source of all the considered  $\text{H}_2^{18}\text{O}$  positions is supposed to be

the W2020 line list [5]. For example, the HITRAN position of the  $13_{113} - 12_{102}$  transition is  $558.84113 \text{ cm}^{-1}$  differs by more than  $10^{-3} \text{ cm}^{-1}$  from its W2020 value ( $558.84022 \text{ cm}^{-1}$  [5]). Our measured value of  $558.84025 \text{ cm}^{-1}$  coincides to the original W2020 value. The *rms* deviation of the present SOLEIL line positions from those of HITRAN2020 is  $1.57 \times 10^{-4} \text{ cm}^{-1}$  for all 565 assigned  $\text{H}_2^{18}\text{O}$  transitions

In the case of the  $\text{H}_2^{17}\text{O}$  isotopologue, for an unknown reason, the W2020 source was rejected for 83 transitions: five and 78 position values were taken from Lodi and Tennyson [28] and updated IUPAC-TG values [41], respectively. Five examples of deviations between the HITRAN  $\text{H}_2^{17}\text{O}$  positions and the SOLEIL spectra are presented in Fig. 9 (one additional panel concerns  $\text{HD}^{16}\text{O}$ ). Interestingly, the original W2020 line positions of Ref. [5] of all

the problematic  $\text{H}_2^{17}\text{O}$  lines agree very well with the experimental spectrum. Note that the HITRAN positions of the lines near 319.71 and 320.12  $\text{cm}^{-1}$  are due to Lodi and Tennyson [28] while the W2020 source is given for the three other  $\text{H}_2^{17}\text{O}$  lines. For the 78 positions with IUPAC-TG origin, the average position difference compared to our measurements is  $1.09 \times 10^{-4} \text{ cm}^{-1}$  with a large *rms* deviation of  $2.87 \times 10^{-3} \text{ cm}^{-1}$ . These values are reduced to  $5.06 \times 10^{-5} \text{ cm}^{-1}$  and  $1.79 \times 10^{-4} \text{ cm}^{-1}$  for the corresponding W2020 values, respectively, indicating that overall, the corresponding W2020 position values of Ref. [5] should have been preferred.

#### 4. Concluding remarks

A series of five high quality FTS spectra of natural water at room temperature has been recorded in the far infrared region using the SOLEIL synchrotron radiation source combined with a cell providing a 151.75-m absorption pathlength. The spectral coverage (50–720  $\text{cm}^{-1}$ ), the high position accuracy (on the order of and  $5 \times 10^{-5} \text{ cm}^{-1}$  for isolated lines of intermediate intensity), and the high sensitivity of the recorded spectra make them valuable for stringent validation tests of spectroscopic databases. An experimental list of more than 3000 transitions of six water isotopologues ( $\text{H}_2^{16}\text{O}$ ,  $\text{H}_2^{17}\text{O}$ ,  $\text{H}_2^{18}\text{O}$ ,  $\text{HD}^{18}\text{O}$ ,  $\text{HD}^{16}\text{O}$ ,  $\text{HD}^{17}\text{O}$ ) were constructed from the five spectra recorded at different pressures up to 7 mbar. The measured line intensities span more than five orders of magnitude. More than 450 lines are newly detected by absorption spectroscopy. The HITRAN2020 [4] and W2020 [5] line lists and the effective Hamiltonian predictions of the  $\text{H}_2^{16}\text{O}$  spectrum by Coudert et al. [6] (14CoMaPi) were compared to the experimental results.

The comparison shows an overall very satisfactory agreement but, even scarce, inaccuracies are of importance as the observed transitions involve rotational levels of the lowest vibrational states – (000), (010) and (020) – which are the lower states of most of the water vapor transitions. Energy levels corrections will thus propagate to calculated line positions in all the energy ranges of the water spectrum. The main results of the comparison can be summarized as follows,

- (i) The 14CoMaPi calculated positions of the main isotopologue agree with the observations within the experimental accuracy,
- (ii) Although the agreement with the W2020 and HITRAN2020 positions is in general very good, a number of transition deviates significantly from the observations. These situations are less numerous in the presently studied rotational range but confirm the conclusion of the validation tests of the W2020 positions in the near infrared region [49] and in the region of the oxygen A-band near 760 nm [48,50]. The evidence of such general problem underlines the necessity of a careful validation tests before implementing the W2020 empirical line positions in reference spectroscopic databases used for atmospheric applications,
- (iii) The uncertainty values attached to the W2020 empirical positions and energy levels can be strongly underestimated. A few examples show deviations exceeding the W2020 uncertainty by factors larger than 10 (up to 459) (see Figs. 6),
- (iv) According to the HITRAN2020 database, the W2020 empirical positions of Ref. [5] were adopted as the main source of line positions in the region. In fact, the HITRAN2020 and the W2020 original line positions do not coincide. As a result, we found series of examples where the position agreement of the recorded spectra was better for HITRAN2020 list than for W2020 list and vice versa (see Figs. 6 and 7),
- (v) Overall, the W2020 line positions of  $\text{H}_2^{17}\text{O}$  show a better agreement with measurements than some HITRAN values and should have been systematically preferred.

Although relatively limited (no new energy levels were determined), the present study has allowed to illustrate the advantage of the state-of-the-art effective Hamiltonian approach for the first vibrational levels of the main isotopologue. Note that only 1310 of the 3001 reported line positions belong to the main isotopologue. Transitions of the minor isotopologues could be used for testing the rotation-bending Hamiltonian developed some years ago for the  $\text{H}_2^{18}\text{O}$  and  $\text{HD}^{16}\text{O}$  species [64,65]. During the measurement campaign of the natural water spectra at SOLEIL, FTS spectra of water samples enriched in  $^{17}\text{O}$  or D (and both) were recorded. The analysis of these spectra will make available a large amount of new information for validation tests of transition frequencies and energy levels of the minor isotopologues (in particular for doubly-substituted species). The obtained results will be reported in separated contributions.

#### Declaration of Competing Interest

The authors declare that they have no known competing financial interests or personal relationships that could have appeared to influence the work reported in this paper.

#### CRediT authorship contribution statement

**M. Toureille:** Investigation. **A.O. Koroleva:** Investigation. **S.N. Mikhailenko:** Investigation. **O. Pirali:** Investigation. **A. Campargue:** Investigation.

#### Acknowledgments

This work became possible due to the Project No 20210051 supported by SOLEIL Synchrotron Team. SNM activity was supported in the frame of the Russian Science Foundation, grant no. 18–11–00024–IT. The support of the CNRS (France) in the frame of International Research Project SAMIA is acknowledged.

#### Supplementary materials

Supplementary material associated with this article can be found, in the online version, at doi:10.1016/j.jqsrt.2022.108326.

#### References

- [1] Mikhailenko SN, Béguier S, Odintsova TA, MYu T, Pirali O, Campargue A. The far-infrared spectrum of  $^{18}\text{O}$  enriched water vapour (40–700  $\text{cm}^{-1}$ ). J Quant Spectrosc Radiat Transf 2020;253:107105. doi:10.1016/j.jqsrt.2020.107105.
- [2] Odintsova TA, MYu T, Zibarova AO, Pirali O, Roy P, Campargue A. Far-infrared self-continuum absorption of  $\text{H}_2^{16}\text{O}$  and  $\text{H}_2^{18}\text{O}$  (15–500  $\text{cm}^{-1}$ ). J Quant Spectrosc Radiat Transf 2019;227:190–200. doi:10.1016/j.jqsrt.2019.02.012.
- [3] Odintsova TA, MYu T, Simonova A, Ptashnik I, Pirali O, Campargue A. Measurement and temperature dependence of the water vapor self-continuum in the 70–700  $\text{cm}^{-1}$  range. J Mol Struct 2020;1210:128046. doi:10.1016/j.molstruc.2020.128046.
- [4] Gordon IE, Rothman LS, Hargreaves RJ, Hashemi R, Karlovets EV, Skinner FM, et al. The HITRAN2020 molecular spectroscopic database. J Quant Spectrosc Radiat Transf 2022;277:107949. doi:10.1016/j.jqsrt.2021.107949.
- [5] Furtenbacher T, Tobias R, Tennyson J, Polyansky OL, Kyuberis AA, Ovsyannikov RI, et al. W2020: a database of validated rovibrational experimental transitions and empirical energy levels of water isotopologues. II.  $\text{H}_2^{17}\text{O}$  and  $\text{H}_2^{18}\text{O}$  with an update to  $\text{H}_2^{16}\text{O}$ . J Phys Chem Ref Data 2020;49:043103. doi:10.1063/5.0030680.
- [6] Coudert LH, Martin-Drumel M-A, Pirali O. Analysis of the high-resolution water spectrum up to the second triad. J Mol Spectrosc 2014;303:36–41. doi:10.1016/j.jms.2014.07.003.
- [7] Kauppinen J, Kärkkäinen T, Kyrö E. High-resolution spectrum of water vapor between 30 and 720  $\text{cm}^{-1}$ . J Mol Spectrosc 1978;71:15–45. doi:10.1016/0022-2852(78)90073-5.
- [8] Kauppinen J, Jolma K, Hornaman VM. New wave-number calibration tables for  $\text{H}_2\text{O}$ ,  $\text{CO}_2$ , and OCS lines between 500 and 900  $\text{cm}^{-1}$ . Appl Opt 1982;21:3332–6. doi:10.1364/AO.21.003332.
- [9] Johns JWC. High-resolution far infrared (20–350  $\text{cm}^{-1}$ ) spectra of several species of  $\text{H}_2\text{O}$ . J Opt Soc Am B 1985;2:1340–54. doi:10.1364/JOSAB.2.001340.

- [10] Paso R, Horneman VM. High-resolution rotational absorption spectra of  $\text{H}_2^{16}\text{O}$ ,  $\text{HD}^{16}\text{O}$ , and  $\text{D}_2^{16}\text{O}$  between 110 and  $500\text{ cm}^{-1}$ . *J Opt Soc Am B* 1995;12:1813–38. doi:[10.1364/JOSAB.12.001813](https://doi.org/10.1364/JOSAB.12.001813).
- [11] Matsushima F, Odashima H, Iwasaki T, Tsunekawa S, Takagi K. Frequency measurement of pure rotational transition of  $\text{H}_2\text{O}$  from 0.5 to 5 THz. *J Mol Struct* 1995;352:371–8. doi:[10.1016/0022-2866\(94\)08531-L](https://doi.org/10.1016/0022-2866(94)08531-L).
- [12] De Natale P, Lorini L, Inguscio M, Nolt IG, Park JH, Di Leonardo G, et al. Accurate frequency measurements for  $\text{H}_2\text{O}$  and  $^{16}\text{O}_3$  in the  $119\text{-cm}^{-1}$  OH atmospheric window. *Appl Opt* 1997;36:8526–32. doi:[10.1364/AO.36.008526](https://doi.org/10.1364/AO.36.008526).
- [13] Toth RA. Water vapor measurements between 590 and  $2582\text{ cm}^{-1}$ : line positions and strengths. *J Mol Spectrosc* 1998;190:379–96. doi:[10.1006/jmsp.1998.7611](https://doi.org/10.1006/jmsp.1998.7611).
- [14] Chen P, Pearson JC, Pickett HM, Matsuura S, Blake GA. Submillimeter-wave measurements and analysis of the ground and  $\nu_2=1$  states of water. *Astrophys J Suppl Series* 2000;128:371–85. doi:[10.1086/313377](https://doi.org/10.1086/313377).
- [15] Horneman VM, Anttila R, Alanko S, Pietilä J. Transferring calibration from  $\text{CO}_2$  laser lines to far infrared water lines with the aid of the  $\nu_2$  band of OCS and the  $\nu_2$ ,  $\nu_1-\nu_2$ , and  $\nu_1+\nu_2$  bands of  $^{13}\text{CS}_2$ : molecular constants of  $^{13}\text{CS}_2$ . *J Mol Spectrosc* 2005;234:238–54. doi:[10.1016/j.jms.2005.09.011](https://doi.org/10.1016/j.jms.2005.09.011).
- [16] Matsushima F, Tomatsu N, Nagai T, Moriwaki Y, Takagi K. Frequency measurement of pure rotational transitions in the  $\nu_2=1$  state of  $\text{H}_2\text{O}$ . *J Mol Spectrosc* 2006;235:190–5. doi:[10.1016/j.jms.2005.11.003](https://doi.org/10.1016/j.jms.2005.11.003).
- [17] Cazzolli G, Pizzarini C, Buffa G, Tarrini O. Pressure-broadening of water lines in the THz frequency region: improvements and confirmations for spectroscopic databases. Part II. *J Quant Spectrosc Radiat Transf* 2009;110:609–18. doi:[10.1016/j.jqsrt.2008.12.001](https://doi.org/10.1016/j.jqsrt.2008.12.001).
- [18] Drouin BJ, Yu SS, Pearson JC, Gupta H. Terahertz spectroscopy for space applications: 2.5–2.7 THz spectra of HD,  $\text{H}_2\text{O}$  and  $\text{NH}_3$ . *J Mol Structure* 2011;1006:2–12. doi:[10.1016/j.molstruc.2011.05.062](https://doi.org/10.1016/j.molstruc.2011.05.062).
- [19] Yu SS, Pearson JC, Drouin BJ, Martin-Drumel M-A, Pirali O, Vervloet M, et al. Measurement and analysis of new terahertz and far-infrared spectra of high temperature water. *J Mol Spectrosc* 2012;279:16–25. doi:[10.1016/j.jms.2012.07.011](https://doi.org/10.1016/j.jms.2012.07.011).
- [20] Yu SS, Pearson JC, Drouin BJ. Terahertz spectroscopy of water in its second triad. *J Mol Spectrosc* 2013;288:7–10. doi:[10.1016/j.jms.2013.03.011](https://doi.org/10.1016/j.jms.2013.03.011).
- [21] Markov VN. Temperature dependence of self-induced pressure broadening and shift of the  $6_{43}-5_{50}$  line of the water molecule. *J Mol Spectrosc* 1994;164:233–8. doi:[10.1006/jmsp.1994.1069](https://doi.org/10.1006/jmsp.1994.1069).
- [22] Markov VN, Krupnov AF. Measurements of the pressure shift of the  $1_{10}-1_{01}$  water line at 556GHz produced by mixtures gases. *J Mol Spectrosc* 1995;172:211–14. doi:[10.1006/jmsp.1995.1168](https://doi.org/10.1006/jmsp.1995.1168).
- [23] Toth RA, Brown LR, Plymate C. Self-broadened widths and frequency shifts of water vapor lines between 590 and  $2400\text{ cm}^{-1}$ . *J Quant Spectrosc Radiat Transf* 1998;59:529–62. doi:[10.1006/jmsp.1995.1168](https://doi.org/10.1006/jmsp.1995.1168).
- [24] Zou Q, Varanasi P. Laboratory measurement of the spectroscopic line parameters of water vapor in the 610–2100 and 3000–4050  $\text{cm}^{-1}$  regions at lower-tropospheric temperatures. *J Quant Spectrosc Radiat Transf* 2003;82:45–98. doi:[10.1006/jmsp.1995.1168](https://doi.org/10.1006/jmsp.1995.1168).
- [25] Podobedov VB, Plusquellic DF, Fraser GT. THz laser study of self-pressure and temperature broadening and shifts of water vapor lines for pressures up to 1.4kPa. *J Quant Spectrosc Radiat Transf* 2004;87:377–85. doi:[10.1016/j.jqsrt.2004.03.001](https://doi.org/10.1016/j.jqsrt.2004.03.001).
- [26] GYu G. Shifting and broadening parameters of the water vapour 183-GHz line ( $3_{13}-2_{20}$ ) by  $\text{H}_2\text{O}$ ,  $\text{O}_2$ ,  $\text{N}_2$ ,  $\text{CO}_2$ ,  $\text{H}_2$ , He, Ne, Ar, and Kr at room temperature. *J Mol Spectrosc* 2005;230:196–8. doi:[10.1016/j.jms.2004.10.011](https://doi.org/10.1016/j.jms.2004.10.011).
- [27] Koshelev MA, MYU T, GYu G, Parshin VV, Markov VN, Koval IA. Broadening and shifting of the 321-, 325- and 380-GHz lines of water vapor by pressure of atmospheric gases. *J Mol Spectrosc* 2007;241:101–8. doi:[10.1016/j.jms.2006.11.005](https://doi.org/10.1016/j.jms.2006.11.005).
- [28] Lodi L, Tennyson J. Line lists for  $\text{H}_2^{18}\text{O}$  and  $\text{H}_2^{17}\text{O}$  based on empirical line positions and *ab initio* intensities. *J Quant Spectrosc Radiat Transf* 2012;113:850–8. doi:[10.1016/j.jqsrt.2012.02.023](https://doi.org/10.1016/j.jqsrt.2012.02.023).
- [29] Coudert LH, Pirali O, Vervloet M, Lanquetin R, Camy-Peyret C. The eight first vibrational states of the water molecule: measurements and analysis. *J Mol Spectrosc* 2004;228:471–98. doi:[10.1016/j.jqsrt.2012.02.023](https://doi.org/10.1016/j.jqsrt.2012.02.023).
- [30] Polyansky OL, Busler JR, Guo B, Zhang K, Bernath PF. The emission spectrum of hot water in the region between 370 and  $930\text{ cm}^{-1}$ . *J Mol Spectrosc* 1996;176:305–15. doi:[10.1006/jmsp.1996.0091](https://doi.org/10.1006/jmsp.1996.0091).
- [31] Polyansky OL, Tennyson J, Bernath PF. The spectrum of hot water: rotational transitions and difference bands in the (020), (100), and (001) vibrational states. *J Mol Spectrosc* 1997;186:213–21. doi:[10.1006/jmsp.1997.7443](https://doi.org/10.1006/jmsp.1997.7443).
- [32] Polyansky OL, Zobov NF, Viti S, Tennyson J, Bernath PF, Wallace L. High-temperature rotational transitions of water in sunspot and laboratory spectra. *J Mol Spectrosc* 1997;186:422–47. doi:[10.1006/jmsp.1997.7449](https://doi.org/10.1006/jmsp.1997.7449).
- [33] Coheur P-F, Bernath PF, Carleer M, Colin R, Polyansky OL, Zobov NF, et al. A 3000K laboratory emission spectrum of water. *J Chem Phys* 2005;122:074307. doi:[10.1063/1.1847571](https://doi.org/10.1063/1.1847571).
- [34] Benedict WS, Pollack MA, Tomlinson WJ III. The water-vapor laser. *IEEE J Quant Electronics* 1969;QE-5:108–24. doi:[10.1109/JQE.1969.1075731](https://doi.org/10.1109/JQE.1969.1075731).
- [35] Winther F. The rotational spectrum of water between 650 and  $50\text{ cm}^{-1}$   $\text{H}_2^{18}\text{O}$  and  $\text{H}_2^{17}\text{O}$  in natural abundance. *J Mol Spectrosc* 1977;65:405–19. doi:[10.1016/0022-2852\(77\)90280-6](https://doi.org/10.1016/0022-2852(77)90280-6).
- [36] Kauppinen J, Kyrö E. High resolution pure rotational spectrum of water vapor enriched by  $\text{H}_2^{17}\text{O}$  and  $\text{H}_2^{18}\text{O}$ . *J Mol Spectrosc* 1980;84:405–23. doi:[10.1016/0022-2852\(80\)90032-6](https://doi.org/10.1016/0022-2852(80)90032-6).
- [37] Matsushima F, Nagase H, Nakauchi T, Odashima H, Takagi K. Frequency measurement of pure rotational transitions of  $\text{H}_2^{17}\text{O}$  and  $\text{H}_2^{18}\text{O}$  from 0.5 to 5 THz. *J Mol Spectrosc* 1999;193:217–23. doi:[10.1006/jmsp.1998.7736](https://doi.org/10.1006/jmsp.1998.7736).
- [38] Mikhailenko SN, VIG T, Mellau G. (000) and (010) states of  $\text{H}_2^{18}\text{O}$ : analysis of rotational transitions in hot emission spectrum in the 400–850  $\text{cm}^{-1}$  region. *J Mol Spectrosc* 2003;217:195–211. doi:[10.1016/S0022-2852\(02\)00018-8](https://doi.org/10.1016/S0022-2852(02)00018-8).
- [39] Toth RA. HDO and  $\text{D}_2\text{O}$  low pressure, long path spectra in the 600–3100  $\text{cm}^{-1}$  region. I. HDO line positions and strengths. *J Mol Spectrosc* 1999;195:73–97. doi:[10.1006/jmsp.1999.7814](https://doi.org/10.1006/jmsp.1999.7814).
- [40] Janca A, Tereszchuk K, Bernath PF, Zobov NF, Shirin SV, Polyansky OL, Tennyson J. Emission spectrum of hot HDO below  $4000\text{ cm}^{-1}$ . *J Mol Spectrosc* 2003;219:132–5. doi:[10.1016/S0022-2852\(03\)00015-8](https://doi.org/10.1016/S0022-2852(03)00015-8).
- [41] Tennyson J, Bernath PF, Brown LR, Campargue A, Carleer MR, Császár AG, et al. IUPAC critical evaluation of the rotational-vibrational spectra of water vapor. Part I – energy levels and transition wavenumbers for  $\text{H}_2^{17}\text{O}$  and  $\text{H}_2^{18}\text{O}$ . *J Quant Spectrosc Radiat Transf* 2009;110:573–96. doi:[10.1016/j.jqsrt.2009.02.014](https://doi.org/10.1016/j.jqsrt.2009.02.014).
- [42] Tennyson J, Bernath PF, Brown LR, Campargue A, Császár AG, Daumont L, et al. IUPAC critical evaluation of the rotational-vibrational spectra of water vapor. Part II: energy levels and transition wavenumbers for  $\text{HD}^{16}\text{O}$ ,  $\text{HD}^{17}\text{O}$ , and  $\text{HD}^{18}\text{O}$ . *J Quant Spectrosc Radiat Transf* 2010;111:2160–84. doi:[10.1016/j.jqsrt.2010.06.012](https://doi.org/10.1016/j.jqsrt.2010.06.012).
- [43] Tennyson J, Bernath PF, Brown LR, Campargue A, Császár AG, Daumont L, et al. IUPAC critical evaluation of the rotational-vibrational spectra of water vapor, Part III. Energy levels and transition wavenumbers for  $\text{H}_2^{16}\text{O}$ . *J Quant Spectrosc Radiat Transf* 2013;117:29–58. doi:[10.1016/j.jqsrt.2012.10.002](https://doi.org/10.1016/j.jqsrt.2012.10.002).
- [44] Tennyson J, Bernath PF, Brown LR, Campargue A, Császár AG, Daumont L, et al. IUPAC critical evaluation of the rotational-vibrational spectra of water vapor. Part IV. Energy levels and transition wavenumbers for  $\text{D}_2^{16}\text{O}$ ,  $\text{D}_2^{17}\text{O}$ , and  $\text{D}_2^{18}\text{O}$ . *J Quant Spectrosc Radiat Transf* 2014;142:93–108. doi:[10.1016/j.jqsrt.2014.03.019](https://doi.org/10.1016/j.jqsrt.2014.03.019).
- [45] Tennyson J, Tobias R, Tennyson J, Polyansky OL, Császár AG. W2020: a database of validated rovibrational experimental transitions and empirical energy levels for  $\text{H}_2^{16}\text{O}$ . *J Phys Chem Ref Data* 2020;49:033101. doi:[10.1063/5.0008253](https://doi.org/10.1063/5.0008253).
- [46] Tobias R, Furtenbacher T, Császár AG. Cycle bases to the rescue. *J Quant Spectrosc Radiat Transf* 2017;203:557–64. doi:[10.1016/j.jqsrt.2017.03.031](https://doi.org/10.1016/j.jqsrt.2017.03.031).
- [47] Tobias R, Furtenbacher T, Tennyson J, Császár AG. Accurate empirical rovibrational energies and transitions of  $\text{H}_2^{16}\text{O}$ . *Phys Chem Chem Phys* 2019;21:3473–95. doi:[10.1039/C8CP05169K](https://doi.org/10.1039/C8CP05169K).
- [48] Vasilchenko S, Mikhailenko SN, Campargue A. Water vapor absorption in the region of the oxygen A-band near 760nm. *J Quant Spectrosc Radiat Transf* 2021;275:107847. doi:[10.1016/j.jqsrt.2021.107847](https://doi.org/10.1016/j.jqsrt.2021.107847).
- [49] Campargue A, Mikhailenko SN, Kassi S, Vasilchenko S. Validation tests of the W2020 energy levels of water vapor. *J Quant Spectrosc Radiat Transf* 2021;276:107914. doi:[10.1016/j.jqsrt.2021.107914](https://doi.org/10.1016/j.jqsrt.2021.107914).
- [50] Vasilchenko S, Mikhailenko SN, Campargue A. Cavity ring down spectroscopy of water vapor near 750 nm: a test of the HITRAN2020 and W2020 line lists. *Mol Phys* 2022;120:e2051762. doi:[10.1080/00268976.2022.2051762](https://doi.org/10.1080/00268976.2022.2051762).
- [51] Esplin MP, Watson RB, Hoke ML, Rothman LS. High-temperature spectrum of  $\text{H}_2\text{O}$  in the 720–1400  $\text{cm}^{-1}$  region. *J Quant Spectrosc Radiat Transf* 1998;60:711–39. doi:[10.1016/S0022-4073\(98\)00079-X](https://doi.org/10.1016/S0022-4073(98)00079-X).
- [52] Zobov NF, Polyansky OL, Tennyson J, Lotoski JA, Calaruso P, Zhang KQ, Bernath PF. Hot bands of water up to  $6\nu_2-5\nu_2$  in the 933–2500  $\text{cm}^{-1}$  region. *J Mol Spectrosc* 1999;193:118–36. doi:[10.1006/jmsp.1998.7732](https://doi.org/10.1006/jmsp.1998.7732).
- [53] Zobov NF, Polyansky OL, Tennyson J, Shirin SV, Nassar R, Hirao T, et al. Using laboratory spectroscopy to identify lines in the K- and L-band spectrum of water in a sunspot. *Astrophys J* 2000;530:994–8. doi:[10.1086/308419](https://doi.org/10.1086/308419).
- [54] Tereszchuk K, Bernath PF, Zobov NF, Shirin SV, Polyansky OL, Libeskind NI, et al. Laboratory spectroscopy of hot water near 2 microns and sunspot spectroscopy in the H-band region. *Astrophys J* 2002;577:496–500. doi:[10.1086/342167](https://doi.org/10.1086/342167).
- [55] Zobov NF, Shirin SV, Polyansky OL, Barber RJ, Tennyson J, Coheur P-F, et al. Spectrum of hot water in the 2000–4750  $\text{cm}^{-1}$  frequency range. *J Mol Spectrosc* 2006;237:115–22. doi:[10.1016/j.jms.2006.03.001](https://doi.org/10.1016/j.jms.2006.03.001).
- [56] Zobov NF, Shirin SV, Ovsyannikov RI, Polyansky OL, Barber RJ, Tennyson J, et al. Spectrum of hot water in the 4750–13 000  $\text{cm}^{-1}$  wavenumber range (0.769–2.1  $\mu\text{m}$ ). *Mon Not R Astron Soc* 2008;387:1093–8. doi:[10.1111/j.1365-2966.2008.13234.x](https://doi.org/10.1111/j.1365-2966.2008.13234.x).
- [57] Rutkowski L, Foltynowicz A, Schmidt FM, Johansson AC, Khodabakhsh A, Kyuberis AA, et al. An experimental water line list at 1950K in the 6250–6670  $\text{cm}^{-1}$  region. *J Quant Spectrosc Radiat Transf* 2018;205:213–19. doi:[10.1016/j.jqsrt.2017.10.016](https://doi.org/10.1016/j.jqsrt.2017.10.016).
- [58] Czinki E, Furtenbacher T, Császár AG, Eckhardt AK, GCh M. The 1943K emission spectrum of  $\text{H}_2^{16}\text{O}$  between 6600 and 7050  $\text{cm}^{-1}$ . *J Quant Spectrosc Radiat Transf* 2018;206:46–54. doi:[10.1016/j.jqsrt.2017.10.028](https://doi.org/10.1016/j.jqsrt.2017.10.028).
- [59] Flaud J-M, Camy-Peyret C, Maillard JP. Higher ro-vibrational levels of  $\text{H}_2\text{O}$  deduced from high resolution oxygen-hydrogen flame spectra between 2800–6200  $\text{cm}^{-1}$ . *Mol Phys* 1976;32:499–521. doi:[10.1080/0026897600103251](https://doi.org/10.1080/0026897600103251).



- [60] Pine AS, Coulombe MJ, Camy-Peyret C, Flaud J-M. Atlas of the high-temperature water vapor spectrum in the 3000–4000  $\text{cm}^{-1}$  region. *J Phys Chem Ref Data* 1983;12:413–65. doi:[10.1063/1.555689](https://doi.org/10.1063/1.555689).
- [61] Dana V, Mandin J-Y, Camy-Peyret C, Flaud J-M, Rothman LS. Rotational and vibrational dependences of collisional linewidths in the  $n\nu_2-(n-1)\nu_2$  hot bands of  $\text{H}_2\text{O}$  from Fourier-transform flame spectra. *Appl Opt* 1992;31:1179–94. doi:[10.1364/AO.31.001179](https://doi.org/10.1364/AO.31.001179).
- [62] Lanquetin R, Coudert LH, Camy-Peyret C. High-lying rotational levels of water: an analysis of the energy levels of the five first vibrational states. *J Mol Spectrosc* 2001;206:83–103. doi:[10.1006/jmsp.2001.8300](https://doi.org/10.1006/jmsp.2001.8300).
- [63] Kyuberis AA, Zobov NF, Naumenko OV, Voronin BA, Polyansky OL, Lodi L, et al. Room temperature line lists for deuterated water. *J Quant Spectrosc Radiat Transf* 2017;203:175–85. doi:[10.1016/j.jqsrt.2017.06.026](https://doi.org/10.1016/j.jqsrt.2017.06.026).
- [64] Coudert LH, Chelin P. Line position and line intensity analyses of the high-resolution spectrum of  $\text{H}_2^{18}\text{O}$  up to the first triad and  $J=17$ . *J Mol Spectrosc* 2016;326:130–5. doi:[10.1016/j.jms.2016.01.012](https://doi.org/10.1016/j.jms.2016.01.012).
- [65] Coudert LH. The bending potential energy function of HDO obtained from high-resolution data. *J Mol Spectrosc* 2016;330:112–19. doi:[10.1016/j.jms.2016.07.008](https://doi.org/10.1016/j.jms.2016.07.008).